Euler Equation Simulation of Propeller-Wing Interaction in Transonic Flow

D L Whitfield*
Mississippi State University, Mississippi State, Mississippi
and
A Jameson†
Princeton University, Princeton, New Jersey

A method is presented for the computation of propeller-wing interaction in transonic rotational flow The approach is to use the three dimensional, time dependent Euler equations with force terms included to simulate the propeller Viscous inviscid interaction on the wing surface is included by coupling the three dimensional Euler equations with the two dimensional compressible turbulent inverse integral boundary layer equations Numerical solutions are compared with experimental data for a 32 deg swept supercritical wing without a propeller simulator, a wing with a propeller simulator producing thrust only, and a wing with a propeller simulator producing thrust and swirl in each direction

Introduction

STUDIES indicate that a significant reduction in fuel consumption of transport aircraft can be achieved by advanced technology turboprop or prop fan propulsion systems It is intended that such propulsion systems be used on transonic aircraft Small changes in transonic flow about a wing can cause appreciable change in shock wave strength and location and consequently influence lift, drag, boundary layer growth, separation, etc Because propellers can produce significant changes in the transonic flow about a wing, it is necessary to understand the influence of a propeller slip stream on a supercritical type wing The purpose of this paper is to present a computational fluid dynamic method of simulating three dimensional transonic propeller wing in teraction, including swirl

Most investigations of propeller wing flowfields have been limited to subsonic[1 5] and high subsonic[6] Mach numbers Rizk[7] and Narain[8] have investigated the transonic problem using the potential flow equations A transonic propeller wing interaction flowfield, however, is rotational due to variations in flow properties induced by the propeller, embedded shocks and viscous effects The approach taken herein is to use the three-dimensional, time dependent Euler equations including the energy equation, in order to allow for rotational flow In addition, viscous effects are taken into account by coupling the three-dimensional Euler equations with the two dimensional compressible turbulent inverse integral boun dary layer equations.

The method used to incorporate the influence of a propeller in the Euler equations is described in the following section The Euler equation solver is then briefly discussed followed by an explanation of how viscous inviscid interaction is in cluded in the computational method Finally, numerical results are presented and compared with results from a transonic flow experiment designed to simulate the influence of a propeller on a supercritical wing

Presented as Paper 83 0236 at the AIAA 21st Aerospace Sciences Meeting Reno Nev , Jan 10 13 1983; received June 28, 1983; revision received April 12, 1984

*Professor Department of Aerospace Engineering Member AIAA

†Professor Department of Mechanical and Aerospace Engineering

Propeller Simulation

The integral form of the Euler equations is used herein From these conservation law equations of mass, momentum, and energy, certain jump conditions can be derived for discontinuity surfaces [9] One of the discontinuity surfaces permitted is a shock across which there is mass flow Shocks can be captured in the solution Another discontinuity surface permitted is one whereby there is no mass flow across the surface For this latter discontinuity surface, the jumps in tangential velocity and density across the surface are ar bitrary, but the jump in pressure is zero A jump in energy is permitted, although the jump must satisfy an equation of state [10] Such jump conditions include those necessary to resolve a propeller slipstream Assuming the method of in corporating the influence of the propeller in the Euler equations is adequate (to be explained below), the approach is to capture the slipstream in the solution as opposed to modeling it explicitly

The method used to incorporate the influence of the propeller in the Euler equations is as follows Forces operate

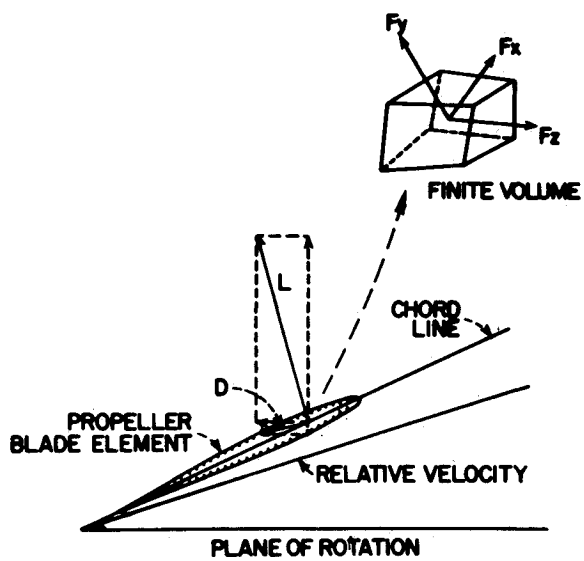

Fig 1 Force diagram of propeller blade element

on the fluid as a consequence of the lift and drag of the blades as illustrated in Fig 1 Because the numerical formulation of the Euler equations used here is finite volume the forces of the blades on the fluid become force vectors associated with the finite volumes located in the propeller region (Fig 1) These finite volume force vectors are variable due to propeller rotation, blade twist, etc

If these finite volume force vectors had resulted from the usual concept of a body force per unit mass, f such as gravitational or electromagnetic forces, then the three dimensional, time dependent Euler equations could be written in Cartesian coordinates for a stationary grid as

$$\int_{V_0} \frac{\partial G}{\partial t} \mathrm{d}V + \int_{S_0} (F_x n_x + F_y n_y + F_z n_z)\,\mathrm{d}S - \int_{V_0} B\,\mathrm{d}V = 0 \tag{1a}$$

where

$$G = [\rho \ \rho u \ \rho v \ \rho w \ \rho E]^T \tag{1b}$$

$$F_x = [\rho u \ \rho uu + p \ \rho vu \ \rho wu \ \rho(E + p/\rho)u]^T \tag{1c}$$

$$F_y = [\rho v \ \rho uv, \rho vv + p \ \rho wv \ \rho(E + p/\rho)v]^T \tag{1d}$$

$$F_z = [\rho w \ \rho uw \ \rho vw \ \rho ww + p \ \rho(E + p/\rho)w]^T \tag{1e}$$

$$B = [0 \ \rho f_x \ \rho f_y, \rho f_z \ \rho(f_x u + f_y v + f_z w)]^T \tag{1f}$$

$$E = \frac{p}{\rho(\gamma - 1)} + \frac{1}{2}(u^2 + v^2 + w^2) \tag{1g}$$

and n_x n_y and n_z are the x y z components of the outward unit normal vector on the surface S enclosing the volume V_0 By applying Eq (1a) to each volume, the result of the integral of B would be a force vector at each cell (finite volume) To account for the effect of a propeller, the cell forces per unit volume are replaced by an equivalent stress system composed of forces per unit area exerted on the cell faces This concept has similarities to that used in magnetohydrodynamics with regard to Maxwell stresses (see, for example, Shercliff[11]) Therefore, because numerical discretization of the last term in Eq (1a) at each cell results in a force in each of the three momentum equations, and each component of force multiplied by the corresponding component of velocity in the energy equation, the influence of the propeller on the flow is regarded as a force per unit area (stress) applied to the cell faces, and numerical treatment of a surface integral rather than a volume integral results in forces occurring in the Euler equations in the same manner as body forces The last term on the left hand side of Eq (1a), therefore, is written in terms of a stress system using Gauss's divergence theorem as

$$\int_{V_0} B\,\mathrm{d}V = \int_{V_0} \mathrm{div}\bar{\tau}\,\mathrm{d}V = \int_{S_0} \tilde{B}\,\mathrm{d}S \tag{2}$$

where

$$\tilde{B} = \bar{\tau}\, n = [0 \ \tilde{f}_x \ \tilde{f}_y \ \tilde{f}_z \ \tilde{f}_x u + \tilde{f}_y v + \tilde{f}_z w]^T \tag{3}$$

and $\tilde{f}$ is a force per unit area

The available experimental transonic flow data of Wedge and Crowder[12] were obtained using a simulator to investigate the effects of a propeller on a supercritical wing Total pressure jumps were introduced by the simulator and vanes were used to induce swirl The thrust was therefore imposed in the present computations by introducing the same jump in total pressure as used in the experiments The force components in the plane perpendicular to the thrust were adjusted to provide the swirl velocities induced by the simulator vanes This was necessary because swirl velocities are not imposed in the computations; rather they are obtained as part of the solution A variation in the stress vector $\tilde{f}$, proportional to the square of the distance from the center of the propeller (or simulator in this case) was used to more appropriately simulate spatial variations

For an actual propeller, the information necessary to specify the stress vector, $\tilde{f}$, might be obtained from the propeller characteristics For example, the components of the stress vector in the thrust direction could be obtained from the distribution of propeller thrust due to the distribution of lift and drag along the blade elements The remaining stress vector components, which are the primary producers of swirl, could be obtained in similar fashion

Euler Equations Solver

The method used to solve the three dimensional time dependent Euler equations with force terms is an extension of that described in Ref 13 Finite volume spatial discretization is applied to the integral form of the Euler equations and the resulting equations are solved using a four stage, two-level numerical scheme The four stage scheme used is second order accurate whereas the four stage scheme used in Ref 13 was fourth order accurate The second order scheme is used because it requires slightly less storage than the fourth order scheme and because steady state solutions are of interest as opposed to time accurate solutions.

Dissipative terms are introduced in this central difference scheme in a separate filter stage at the end of each time step Convergence to a steady state is accelerated by the addition of a forcing term that depends on the difference between the local total enthalpy and the freestream value of enthalpy Convergence is also accelerated by using a local time step determined by the maximum Courant number of $2\sqrt{-2}$ Far-field boundary conditions are based on a characteristic combination of variables [13] Pressure at the wall is determined by a three dimensional version of the work of Rizzi[14] in volving the normal momentum relation

Viscous-Inviscid Interaction

Viscous effects were taken into account in an approximate fashion by coupling the three dimensional Euler equations with the two dimensional compressible turbulent inverse integral boundary layer equations The inverse boundary layer method is described in Ref 15 An inverse method allows for regions of separated flow and the one described in Ref 15 can be used everywhere, whether or not the flow separates

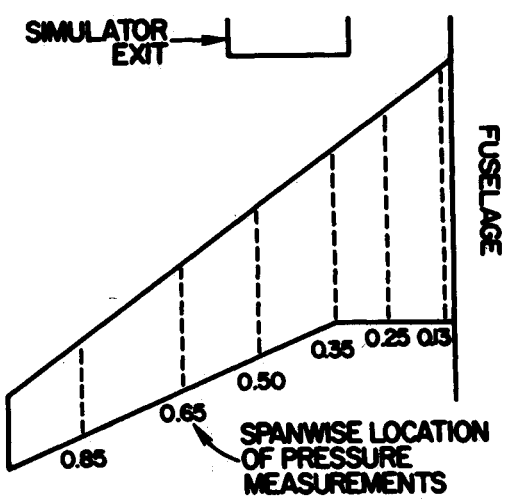

Fig 2 Schematic of simulator and wing

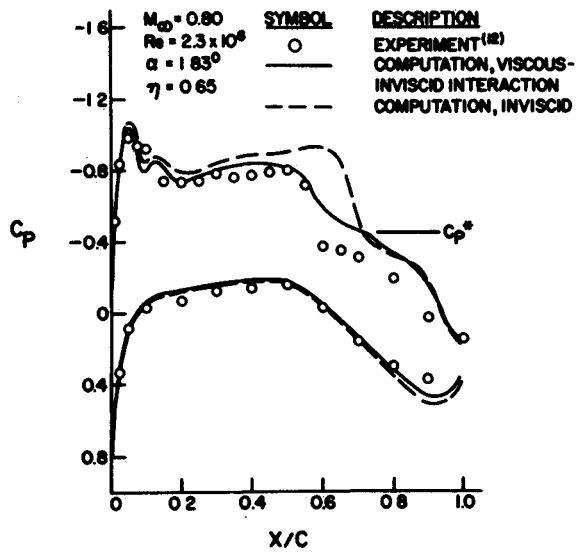

Fig 3 Numerical and experimental wing surface pressures with no simulator and with and without viscous effects

Viscous inviscid interaction solutions were obtained using the surface source method as explained in Refs 16 and 17 This method accounts for interaction by imposing a surface source term in each of the Euler equations as described in Ref 18 The iteration procedure used in Ref 17 was followed except that the boundary layer equations were solved after every 20 time cycles of the Euler equations rather than after every 50 cycles The reason for this is that the time step resulting from the present three dimensional grid ($96\times16\times16$) was larger than that resulting from the finer two dimensional grid (128×30) used in Ref 17 Both the inviscid and viscous inviscid interaction solutions involved 400 Euler equation cycles Carter's method[19] of iterating on the displacement thickness was used, with a relaxation of unity

Boundary layer solutions were obtained over the wing in the freestream direction at each spanwise location Ten cells in the spanwise direction were taken on the wing The boundary layer solutions were started at each span station at the 20% local chord location on the lower surface and the 15% local chord location on the upper surface, as this corresponded to the boundary layer trip locations used in the experiment [12]

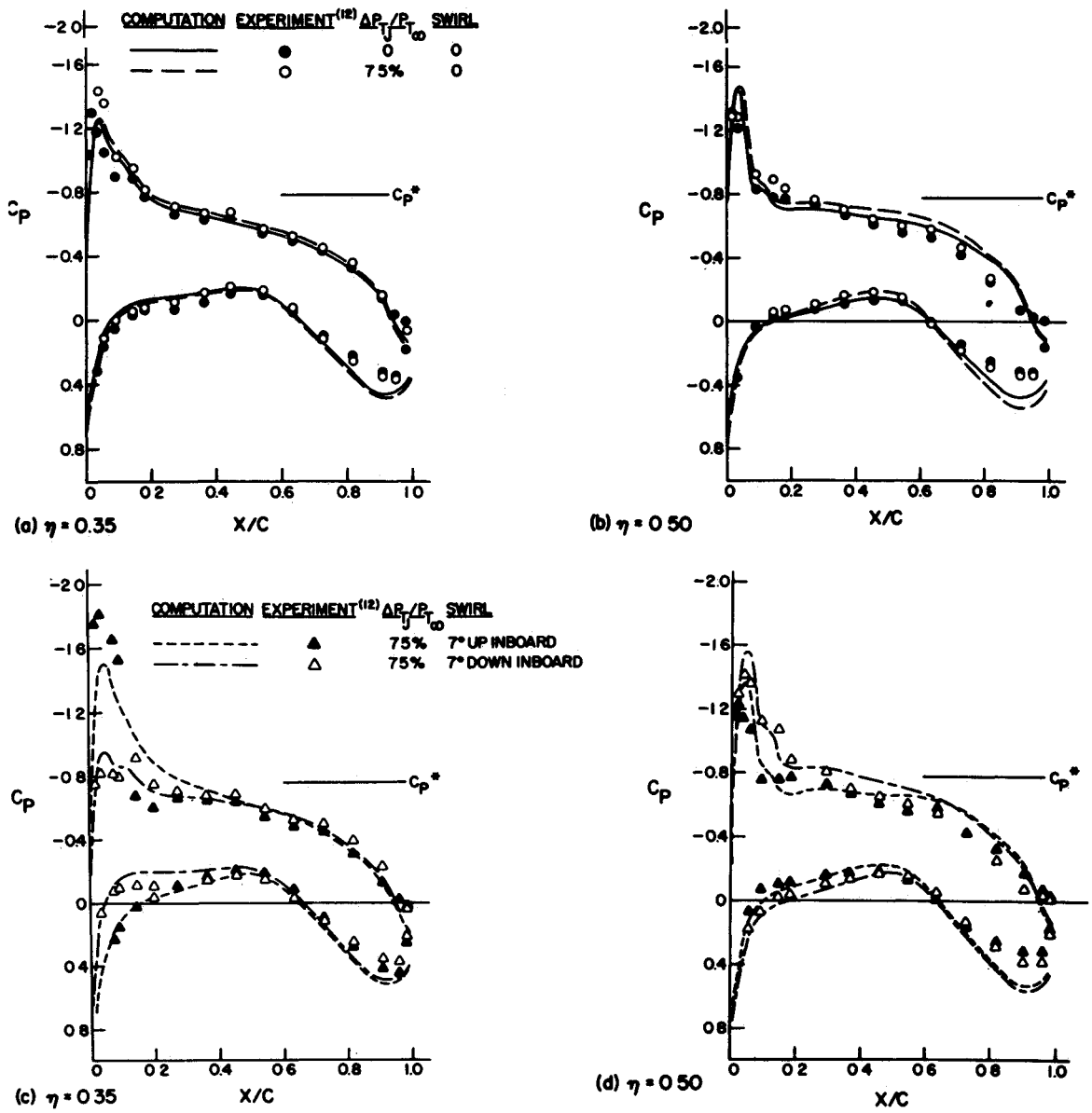

Fig 4 Numerical and experimental wing surface pressures with and without simulator for $M_\infty = 0.70$, $Re = 2.3\times10^6$ and $\alpha = 3$ deg

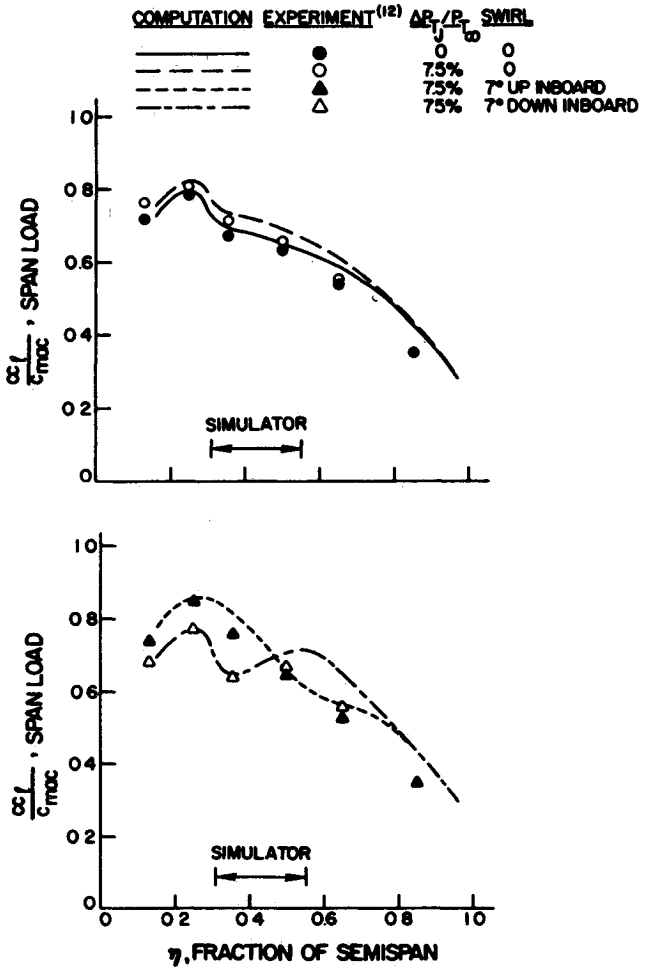

Fig 5 Numerical and experimental spanwise load distributions for $M_\infty = 0\ 80$, $Re = 2\ 3 \times 10^6$, and $\alpha = 3$ deg

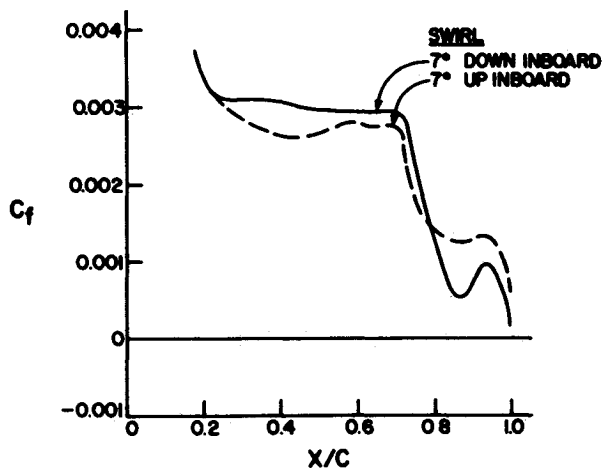

Fig 6 Influence of swirl on the upper surface wing boundary layer at $\eta = 0\ 43$ for $M_\infty = 0\ 80$, $Re = 2\ 3 \times 10^6$, and $\alpha = 3$ deg

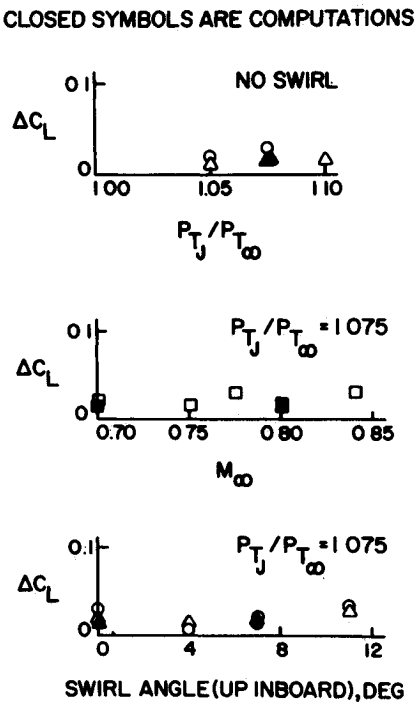

Fig 7 Numerical and experimental incremental lift data for $\alpha = 3$ deg and $Re = 2\ 3 \times 10^6$

Results and Comparisons

Available experimental transonic data appear to be those of Wedge and Crowder [12] This experiment was stated[12] to be of an exploratory nature to identify order of magnitude slip stream wing interaction effects and not to establish highly accurate results A simulator consisting of a high pressure air driven ejector system was used to simulate a modern prop fan slipstream A schematic of the simulator and wing is shown in Fig 2 The simulator exit diameter was 11 7% of the model span The airfoil sections defining the wing are tabulated in Ref 12 This wing has 32 deg of quarter chord sweep and a taper ratio of 0 30

All numerical solutions were obtained on a $96 \times 16 \times 16$ C type grid with 60 points on the wing at each of 11 span locations The experiment used a wing body combination; however the grid was for a wing alone Moreover, for these initial computations no special gridding of the propeller was used The propeller (or simulator) region was, therefore, essentially a rectangle in appearance when viewed from directly upstream or downstream The C type grid did permit a reasonably vertical simulation of the propeller region

An example of viscous inviscid interaction results com pared to purely inviscid results is given in Fig 3 for M_∞ (freestream Mach number) of 0 80, Re (Reynolds number based on mean aerodynamic chord) of $2\ 3 \times 10^6$ α (angle of attack) of 1 83 deg η (semispan location) of 0 65 and no propeller simulator As illustrated in Fig 3, viscous inviscid interaction improves the agreement between the numerical and experimental results by moving the shock location for ward and decreasing the lift in general However this grid is not sufficiently fine to resolve the shock adequately par ticularly over the aft portion of the wing where the grid spacing approaches 6% percent of the local chord The discrepancy on the aft portion of the lower surface exists in all comparisons This may be an indication that three dimensional boundary layer effects not included in these computations, are important.

Comparisons of numerical and experimental wing surface pressures with and without the simulator and with and without the swirl are given in Fig 4 for $M_\infty = 0\ 70$ and $\alpha = 3$ deg The term ΔP_{T_J} is the jump in total pressure at the simulator Results are presented at two span locations, $\eta = 0\ 35$ and 0 50. These span locations were selected because the propeller simulator has the greatest influence on the flow about the wing at these locations (see Fig 2) Figures 4a and b indicate that the propeller simulator changed the wing pressure distribution somewhat as compared to no simulator However Figs 4c and d indicate that swirl, both up inboard and down inboard has a much larger effect Swirl influences the pressure distribution more on the inboard station

($\eta = 0\ 35$) than the outboard station ($\eta = 0.50$) The com putations in Fig 4 include viscous inviscid interaction and are considered to be in reasonable agreement with the ex perimental data

Numerical and experimental span load distributions are presented in Fig 5 for $M_\infty = 0\ 80$ and $\alpha = 3$ deg The span load parameter used in Fig 5, cc_l/c_{mac} is the local lift coefficient c_l times the ratio of the local chord c to the mean aerodynamic chord c_{mac} The most interesting results are those that include swirl Quantitative agreement between theory and experiment is worse on the outboard portion of the wing, although the numerical results are in good qualitative agreement with the experimental data in Fig 5 The com putations include viscous inviscid interaction

The influence of the propeller simulator on the upper wing surface boundary layer for $M_\infty = 0.80$ and $\alpha = 3$ deg is illustrated in Fig 6 Of particular interest is whether or not flow separation occurs as a consequence of the propeller slipstream Although the boundary layer treatment is two dimensional, the inverse method used can predict separated flow The local skin friction coefficient, c_f, is plotted in Fig 6 at $\eta = 0\ 43$ which is the wing span station located downstream of the center of the propeller simulator The influence of 7 deg down inboard swirl as compared to 7 deg up inboard swirl is to strengthen the upper surface shock and move it aft somewhat Although the flow does not separate in the computations with swirl in either direction, the upper surface boundary layer corresponding to the case with 7 deg down inboard swirl is close to separation just downstream of the shock and near the trailing edge due to the stronger shock

Experimental incremental lift coefficients are presented in Ref 12 for various simulator to freestream total pressure ratios (P_{T_J}/P_{t_∞}), freestream Mach numbers, and up inboard swirl angles The lift increments are referenced to $P_{T_J}/P_{T_\infty} = 1\ 000$ and zero swirl Computations for freestream Mach numbers of 0 70 and 0 80, and swirl angles of zero and 7 deg up inboard are compared with experimental data in Fig 7 The computed incremental lift results with viscous inviscid interaction are shown in Fig 7 to be in good agreement with the experimental data

Conclusions

A computational method was presented for solving the three dimensional, time dependent Euler equations with force terms that are similar to body forces These particular force terms were introduced to simulate a propeller In addition viscous effects were accounted for in an approximate fashion by coupling the three dimensional Euler equations with the two dimensional compressible turbulent inverse integral boundary layer equations

Viscous-inviscid interaction computations were carried out for transonic flow about a 32 deg swept supercritical wing with: 1) no influence of a propeller 2) the influence of a propeller producing thrust only, and 3) the influence of a propeller producing both thrust and swirl (in either direction) Although a wing with only one propeller was investigated, there is no restriction on the number of propellers that can be included, nor the direction of swirl produced by each propeller The $96 \times 16 \times 16$ grid used was rather coarse; however, comparisons with experiments indicate the com putational method is a useful tool for investigating this practical three dimensional flow problem with vorticity

All computations were performed on a CRAY 1S computer that had about 900,000 words of available memory A viscous inviscid interaction solution on a $96 \times 16 \times 16$ grid with 400 Euler equation cycles and 20 boundary layer equation cycles required 341 s and the 900 000 words of memory

References

[1] Chow F Krause, E , Liu C H and Mao J Numerical Investigations of an Airfoil in a Non Uniform Stream *Journal of Aircraft* Vol 7, June 1970 pp 531 537

[2] Kleinstein G and Liu C H , Application of Airfoil Theory for Nonuniform Streams to Wing Propeller Interaction *Journal of Aircraft* Vol 19 Feb 1972 pp 137 142

[3] Lan C E Wing Slipstream Interaction with Mach Number Nonuniformity *Journal of Aircraft* Vol 12 Oct 1975 pp 759 760

[4] Shollenberger C A , Three Dimensional Wing/Jet Interaction Analysis Including Jet Distortion Influences, *Journal of Aircraft* Vol 12 Sept 1975 pp 706 713

[5] Ting, L Lin C H and Kleinstein G Interference of Wing and Multipropellers *AIAA Journal* Vol 10 July 1972 pp 906 914

[6] Boctor, M. L Clay C W and Watson C F An Analysis of Prop Fan/Airframe Aerodynamic Integration NASA CR 152186 Oct 1978

[7] Rizk M H Propeller Slipstream/Wing Interaction in the Transonic Regime, Flow Research Rept No 132 Kent, Washington June 1979

[8] Narain J P A Transonic Analysis of Prop Fan Slipstream Effect on a Supercritical Wing AIAA Paper 83 0186 Jan 1983

[9] Jeffrey, A and Taniuti T *Non Linear Wave Propagation* Academic Press New York 1964

[10] MacCormack, R W and Paullay A J The Influence of the Computational Mesh on Accuracy for Initial Value Problems with Discontinuous or Nonunique Solutions *Computers and Fluids* Vol 2 1974 pp 339 361

[11] Shercliff J A , *A Textbook of Magnetohydrodynamics,* Pergamon Press New York 1965

[12] Wedge H R and Crowder, J P Simulated Propeller Slip stream Effects on a Supercritical Wing NASA CR 152138 June 1978

[13] Jameson, A Schmidt, W and Turkel E Numerical Solution of the Euler Equations by Finite Volume Methods Using Runge Kutta Time Stepping Schemes ' AIAA Paper 81 1259 June 1981

[14] Rizzi A Numerical Implementation of Solid Body Boundary Conditions for the Euler Equations ' *ZAMM*, Vol 58 1978 pp 301 304.

[15] Whitfield D L Swafford, T W and Donegan T L , ' An Inverse Integral Computational Method for Compressible Turbulent Boundary Layers in *Recent Contributions to Fluid Mechanics* edited by A Haase Springer Verlag New York 1982 pp 294-302.

[16] Whitfield D L Swafford, T W and Jacocks J L , Calculation of Turbulent Boundary Layers with Separation and Viscous Inviscid Interaction *AIAA Journal* Vol 19 Oct 1981, pp 1315 1322

[17] Schmidt W , Jameson A and Whitfield D Finite Volume Solutions to the Euler Equations in Transonic Flow *Journal of Aircraft* Vol 20 Feb 1983 pp 127 133

[18] Whitfield D Thomas J Jameson A and Schmidt W Computation of Transonic Viscous Inviscid Interacting Flow ' in *Numerical and Physical Aspects of Aerodynamic Flows II* edited by T Cebeci Springer Verlag New York 1984 pp 285 295

[19] Carter J E A New Boundary Layer Inviscid Interaction Technique for Separated Flow AIAA Paper 79 1450 July 1979